Mechanical and chemical bonding properties of ground state BeH_2

Bao-Tian Wang,[1,2] Ping Zhang,[2,*] Hongliang Shi,[3,2] Bo Sun,[2] and Weidong Li[1]

[1] *Institute of Theoretical Physics and Department of Physics, Shanxi University, Taiyuan 030006, People's Republic of China*

[2] *LCP, Institute of Applied Physics and Computational Mathematics, Beijing 100088, People's Republic of China*

[3] *SKLSM, Institute of Semiconductors, Chinese Academy of Sciences, People's Republic of China*

The crystal structure, mechanical properties and electronic structure of ground state BeH_2 are calculated employing the first-principles methods based on the density functional theory. Our calculated structural parameters at equilibrium volume are well consistent with experimental results. Elastic constants, which well obey the mechanical stability criteria, are firstly theoretically acquired. The bulk modulus B, Shear modulus G, Young's modulus E and Poisson's ratio υ are deduced from the elastic constants. The bonding nature in BeH_2 is fully interpreted by combining characteristics in band structure, density of state, and charge distribution. The ionicity in the Be−H bond is mainly featured by charge transfer from Be $2s$ to H $1s$ atomic orbitals while its covalency is dominated by the hybridization of H $1s$ and Be $2p$ states. The valency in BeH_2 can be represented as $Be^{1.99+}H^{0.63-}$, which suggests that significant charge transfer process exists.

PACS numbers: 68.43.Bc, 68.43.Fg, 68.43.Jk, 73.20.Hb

I. INTRODUCTION

There has been a great interest in simple alkali-metal and alkaline-earth-metal hydride systems stimulated by both the fundamental interests and various applications. Such kinds of metal hydrides, e.g., beryllium and magnesium and beryllium-magnesium-based hydrides, which all have high weight percentage of hydrogen, are promising candidates for hydrogen storage. If they become metallic when subjected to high pressures, they may be candidates for high-temperature superconductivity. Among them, MgH_2 has been extensively studied both experimentally and theoretically. Due to the experimental difficulties in material synthesis[1], on the other hand, a comprehensive understanding of BeH_2 is still being in progress. It had long been considered that BeH_2 was a polymer and did not crystallize without ternary additions. Recently, however, Smith *et al.*[2] have successfully synthesized crystalline BeH_2 and first established the crystal structure as the body-centered orthorhombic by synchrotron-radiation-based powder x-ray diffraction. Since this experimental establishment, to date theoretical studies on physical properties of crystalline BeH_2 are very scarce in the literature. Vajeeston *et al.*[3] and Hantsch *et al.*[4] have studied the structural stability of BeH_2 by performing first-principles total-energy calculations for various types of structural variants, among which they confirmed that the experimentally observed BeH_2 modification has the lowest total energy. No further theoretical studies have been reported, although more experimental works are going on to investigate the pressure dependence of physical properties of BeH_2[5].

In this paper, we have carried out the first-principles calculations of ground-state behavior of BeH_2 at its experimentally established crystalline phase. Results for the electronic and atomic structure, mechanical properties, charge density participation, and the nature of Be-H chemical bonding, are systematically presented. Our calculated results for elastic constants indicate that the experimentally observed orthorhombic phase of BeH_2 is mechanically stable. We determined that the ionic charge of Be and H in BeH_2 are represented $Be^{1.99+}$ and $H^{0.63-}$, which, when compared to $Mg^{1.95+}$ and $H^{0.6-}$ in MgH_2, indicates that the charge transfer process in BeH_2 is more prominent in MgH_2.

II. CALCULATION METHOD

The density-functional theory (DFT) total energy calculations for the ground state BeH_2 were carried out using the Vienna *ab initio* simulations package(VASP)[6] with the projected-augmented-wave (PAW) pseudopotentials[7] and plane waves. The generalized gradient approximation (GGA)[8] for the exchange-correlation potential was employed. 7×7×7 Monkhorst-Pack[9] k points in the full wedge of the Brillouin zone were used. The plane-wave energy cutoff was set 500 eV, and all atoms were fully relaxed until the Hellmann-Feynman forces were less than 0.002 eV/Å. To obtain optimized lattice vectors and atomic coordinates of bulk unit cell, we relaxed it at a series of fixed volumes. The bulk modulus B, shear modulus G, Young's modulus E, Poisson's ratio υ, were gained through computing elastic constants.

III. RESULTS AND DISCUSSION

A. Atomic structure and mechanical properties

The ground state of BeH_2, which has been testified both experimentally[2] and theoretically[3], belongs to body-centered orthorhombic structure with space group *Ibam*. Its orthorhombic unit cell is composed of twelve

TABLE I: Calculated structural parameters, bulk modulus B, shear modulus G, Young's modulus E, Poisson's ratio υ and energy band gap (E_g) for orthorhombic BeH_2. As a comparison, other theoretical work and available experimental data are listed.

	Present calculations	Previous calculations	Expt.
a (Å)	9.0049	8.9823	9.082
b (Å)	4.1684	4.1563	4.160
c (Å)	7.6347	7.6455	7.707
V (Å^3)	286.6	285.4	291.2
Coordinates	Be1($4a$): 0, 0, 0.25	0, 0, 0.25	0, 0, 0.25
	Be2($8j$): 0.1684, 0.1199, 0	0.1678, 0.1207, 0	0.1699, 0.1253, 0
	H1($16k$): 0.0881, 0.2216, 0.1516	0.0720, 0.1842, 0.1361	0.0895, 0.1949, 0.1515
	H2($8j$): 0.3092, 0.2792, 0	0.3097, 0.2790, 0	0.3055, 0.2823, 0
Be1-H1 (Å)	1.328	1.435[b]	1.38(2)
Be2-H1 (Å)	1.376		1.41(2)
Be2-H2 (Å)	1.434	1.439[b]	1.44(2)
H1-Be1-H1 (°)	109.6		107.7(5)
H1-Be2-H1 (°)	98.3	98.6[b]	112.1(5)
H1-Be2-H2 (°)	117.9		111.2(5)
H2-Be2-H2 (°)	109.2		109.1(5)
Be1-H1-Be2 (°)	133.6	126.4[b]	130(1)
Be2-H2-Be2 (°)	125.4	120.0[b]	127(1)
B (GPa)	22.60	23.79	14.2±3.0[a]
G (Gpa)	24.50		
E (GPa)	53.99		
υ	0.102		0.21[a]
E_g (eV)	5.52	5.51	

[a]Experimentally measured values from Ref.[5] for amorphous BeH_2 at ambient pressure. Other experimental values are selected from Ref.[2]. [b]Previous theoretical values from Ref.[4] and other from Ref.[3].

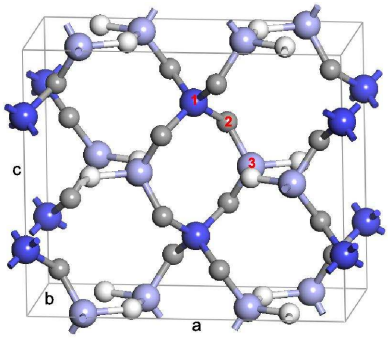

FIG. 1: (Color online) Unit cell for body-centered orthorhombic BeH_2. Both Be and H have two kinds of atomic occupations, which are in the figure presented by blue (Be1), light blue (Be2), gray (H1), and white (H2) spheres.

BeH_2 formula units, see Fig. 1. The primitive cell, containing six formula units, has two Be1 ($4a$, in Wyckoff notation), four Be2 ($8j$), eight H1 ($16k$), and four H2 ($8j$) atoms. Each Be1 is surrounded by four H1 atoms to build the tetrahedral structure and each Be2 connects with two H1 atoms and two H2 atoms. This can be clearly seen from Fig. 1, in which the larger blue spheres stand for Be1 atoms and the larger light blue Be2 while the smaller gray spheres denote H1 atoms and the smaller white H2. Calculated atomic structural parameters for orthorhombic BeH_2 are presented in Table I. As a comparison, the previous theoretical results[3,4] and available experimental data[2,5] are also listed. It is clear that our calculated results are on the whole in good agreement with the experimental data, which thus confirms that the present calculation is reliable and accurate. The exception is that in analogy with previous theoretical report[4], our calculated H1-Be2-H1 bond angle (98.3°) is underestimated by 12% compared with the experimental value (112.1°)[2]. Although it remains unclear for us to explain this discrepancy, we can be sure that it is not caused by the choice of the exchange-correlation potential. In fact, we have found that the use of local density approximation (LDA) even more underestimates the H1-Be2-H1 bond angle.

Elastic constants can measure the resistance and mechanical features of crystal to external stress or pressure, thus describing the stability of crystals. For the present orthorhombic BeH_2, there are nine independent elastic constants, which are in our first-principles calculations obtained by applying small elastic strains. For each time

TABLE II: Calculated elastic constant of BeH_2 (*Ibam*). All values are in units of GPa.

C_{11}	C_{22}	C_{33}	C_{44}	C_{55}	C_{66}	C_{12}	C_{23}	C_{13}
63.85	40.33	89.44	14.69	34.00	21.01	0.63	0.66	10.76

that the strain changes, the coordinates of ions are fully relaxed to ensure the energy minimum rule. In our calculations the strain δ is varied in steps of 0.006 from δ=-0.036 to 0.036. The calculated elastic constants are listed in Table II. Although at present there exist no experimental data to compare with our calculated elastic constants, based on the good agreement between our calculations and the experiment for the atomic structural parameters, we expect that our calculated elastic constants can be adopted in the realistic application if the mechanical data are needed for BeH_2.

The availability of the elastic constants can be used to measure the stability of a specific material. For the orthorhombic crystalline structure, the mechanical stability criteria are given by[10]

$$\begin{aligned} &C_{11}>0, C_{22}>0, C_{33}>0, C_{44}>0, C_{55}>0, C_{66}>0,\\ &[C_{11}+C_{22}+C_{33}+2(C_{12}+C_{13}+C_{23})]>0,\\ &(C_{11}+C_{22}-2C_{12})>0, (C_{11}+C_{33}-2C_{13})>0,\\ &(C_{22}+C_{33}-2C_{23})>0. \end{aligned} \quad (1)$$

From Table II we can see that the orthorhombic BeH_2 is mechanically stable because its elastic constants satisfy formula (1). In fact, the calculated amplitudes of C_{12} and C_{23} are negligibly small, and the amplitude of C_{13} is prominently smaller than that of either C_{11} or C_{33}. Thus, formula (1) is easily satisfied.

After obtaining elastic constants, we can calculate bulk and shear moduli from the Voigt-Reuss-Hill (VRH) approximation[11,12,13]. The Voigt bounds[11,14] on the effective bulk modulus B_V and shear modulus G_V are

$$B_V = (1/9)[C_{11}+C_{22}+C_{33}+2(C_{12}+C_{13}+C_{23})] \quad (2)$$

and

$$\begin{aligned} G_V = (1/15)[&C_{11}+C_{22}+C_{33}+3(C_{44}+C_{55}+C_{66})\\ &-(C_{12}+C_{13}+C_{23})]. \end{aligned} \quad (3)$$

Under Reuss approximation[12], the Reuss bulk modulus B_R and Reuss shear modulus G_R are

$$\begin{aligned} B_R = \Delta[&C_{11}(C_{22}+C_{33}-2C_{23})+C_{22}(C_{33}-2C_{13})\\ &-2C_{33}C_{12}+C_{12}(2C_{23}-C_{12})+C_{13}(2C_{12}-C_{13})\\ &+C_{23}(2C_{13}-C_{23})]^{-1} \end{aligned} \quad (4)$$

and

$$\begin{aligned} G_R = 15\{4[&C_{11}(C_{22}+C_{33}+C_{23})+C_{22}(C_{33}+C_{13})\\ &+C_{33}C_{12}-C_{12}(C_{23}+C_{12})-C_{13}(C_{12}+C_{13})\\ &-C_{23}(C_{13}+C_{23})]/\Delta+3[(1/C_{44})+(1/C_{55})\\ &+(1/C_{66})]\}^{-1}, \end{aligned} \quad (5)$$

where

$$\begin{aligned} \Delta = &C_{13}(C_{12}C_{23}-C_{13}C_{22})+C_{23}(C_{12}C_{13}\\ &-C_{23}C_{11})+C_{33}(C_{11}C_{22}-C_{12}^2). \end{aligned} \quad (6)$$

The bulk modulus B and shear modulus G, based on Hill approximation[13], are arithmetic average of Voigt and Reuss elastic modulus, i.e., B=$\frac{1}{2}(B_R+B_V)$ and G=$\frac{1}{2}(G_R+G_V)$. The Young's modulus E and Poisson's ratio υ for an isotropic material are given by[15]

$$E = \frac{9BG}{3B+G}$$

and

$$\upsilon = \frac{3B-2G}{2(3B+G)}.$$

The calculated results for these moduli and Poisson's ratio are listed in Table I. Note that we have also calculated the bulk modulus B by fitting the Murnaghan equation of state. The derived bulk modulus is well comparable with that from the above VRH approximation, which again indicates that our calculations are consistent and reliable. We find that the bulk modulus of BeH_2 is much smaller than that of MgH_2 (previous first-principles reports[19,20] gave B∼50 GPa in the MgH_2 system), which means that BeH_2 is more easily compressed. The reason is that the rutile structure of MgH_2 is more dense in atomic packing than the body-centered orthorhombic structure of BeH_2. Although at present no experimental data for these moduli and Poisson's ratio are attainable for pure BeH_2, recent Brillouin scattering experiment[5] on amorphous BeH_2 gave B=14.2±3.0 GPa and υ=0.21. Considering the fact that the amorphous BeH_2 is more loose than the pure BeH_2, it is understandable that our calculated modulus for the pure phase is larger than the experimental measurement for the amorphous phase. Concerning the Poisson's ratio, our calculated υ=0.102 for the pure BeH_2 is much smaller than the experimental measurement on the amorphous phase. This is also really understandable. In fact, it is well known that for the common materials that have much smaller shear moduli compared with the bulk moduli, their Poisson's ratio is close to 1/3. If the shear modulus, on the other hand, is much larger than the bulk modulus, materials will have negative Poisson's ratio[16]. In the case of BeH_2, our calculated results in Table I show that the shear modulus is comparable to the bulk modulus. Then, it is anticipated that the Poisson's ratio of the orthorhombic BeH_2 has a small value, which is consistent with our calculated result of υ=0.102. The experimentally measured larger Poisson's ratio[5] is therefore due to the use of amorphous sample.

B. Electronic structure and charge distribution

The calculated band structure of BeH_2 is shown in Fig. 2. Our theoretical valence-band width is 6.5 eV

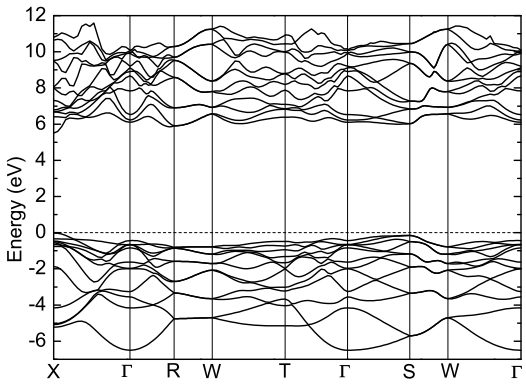

FIG. 2: GGA band structure of BeH_2. The Fermi energy is set at zero.

and band gap 5.5 eV, which is consistent with previous calculation[3]. As an illustrating comparison, in isoelectronic MgH_2 the calculated valence-band width is 7.5 eV and band gap 4.2 eV[17], which implicitly suggests that the Mg−H bond is more ionic than the Be−H bond. Also one can see from Fig. 2 that the valence band maximum (VBM) and conduction band minimum (CBM) both appear at **X** point in the Brillouin zone. By calculating the orbital-decomposed band charges inside the muffin-tin spheres of BeH_2 at VBM and CBM at **X** point, we find that the VBM has predominant H 1s state character mixed with significant Be 2p contribution, while the CBM has obvious Be 2s and 2p features mixed with a little H 1s contribution.

The total electronic density of states (DOS) per unit cell for the orthorhombic BeH_2 is shown in Fig. 3(a). For more clear illustration, the orbital-resolved partial DOS per atom in the unit cell are also shown in Fig. 3, see Fig. 3(b) for H1 and H2 atoms, and Fig. 3(c) for Be1 and Be2 atoms. From Fig. 3 the following prominent features can be seen: (i) H 1s state hybridizes with Be 2s and 2p states in the whole range of the valence band. This is different from alkali-metal hydrides. Due to the combined fact that there has only one valence electron with low ionization energy and the $s \rightarrow p$ promotion energy is relatively large in alkali-metal elements, usually alkali-metal hydrides have entire ionic bonding in the sense that the valence electrons in alkali-metal atoms totally transfer to the H atoms. This clear ionic picture in alkali-metal hydrides becomes blurred in alkaline-earth-metal hydrides. In the present case of BeH_2, in addition to a large ionic weight (see the following charge-distribution analysis), a distinct covalent component also exists in the Be−H bond, which is responsible for the stabilization of the low symmetric structure of BeH_2. Prominently, this covalency is dominated by the hybridization of H 1s and Be 2p orbitals near the top of the valence band, while the hybridization of H 1s and Be 2s orbitals is relatively weak, as shown in Fig. 3. Thus, the ionicity in the Be−H bond is mainly featured by charge transfer from Be 2s to H

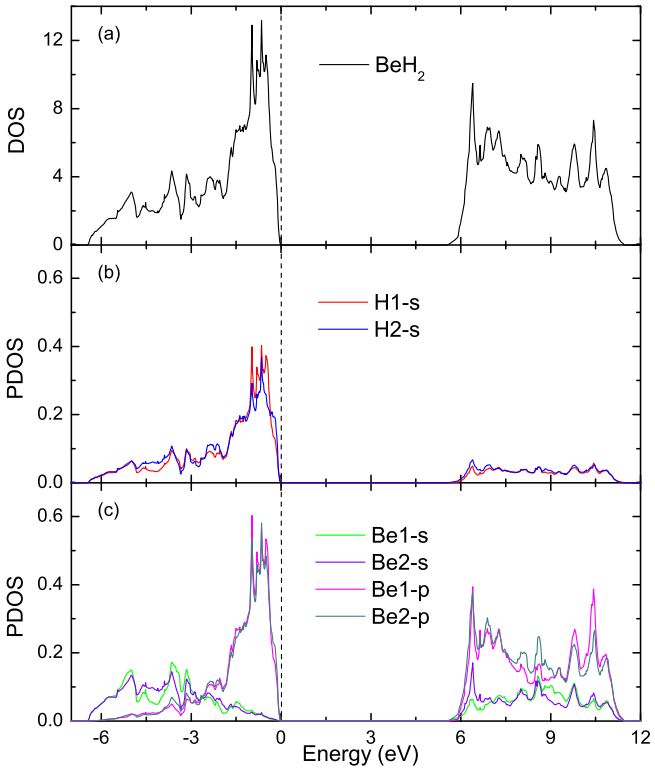

FIG. 3: (Color online) Total and orbital-resolved local densities of states for ground state BeH_2. The Fermi energy is set at zero.

1s atomic orbitals. Interestingly, in beryllium oxide the Be−O bond also exhibits strong covalency. As a result, bulk BeO has wurtzite structure instead of the usual form of rocksalt structure taken by other alkaline-earth-metal oxides; (ii) In the range of conduction band the DOS is mainly featured by Be 2s and 2p states, mixed with a little H 1s states; (iii) Although there are three Be−H bond configurations (Be1−H1, B1−H2, and Be2−H2), the DOS propertie of these chemical bonds are almost the same and there is no remarkable difference between Be1 and Be2 (or between H1 and H2) atoms.

In order to gain more insight into the nature of Be−H chemical bonding in the orthorhombic BeH_2, we have investigated the valence charge density distribution. Two contour plots of the valence charge density distributions are shown in Fig. 4. Here the contour plane in Fig. 4(a) is the plane composed by the three labeled atoms (1 to 3) shown in Fig. 1, while the contour plane in Fig. 4(b) is the (001) plane (perpendicular to the c axis). It is these two planes that characterize the bond structure of BeH_2. In both planes, hydrogen charge density shape is deformed toward the direction to the nearest-neighbor Be atoms. The charge density around H atoms is higher than that around Be atoms. This further indicates aforementioned significant ionic-type charge transfer from Be 2s to H 1s state. On the other hand, the charge densities at the midpoint of Be−H bond is 0.46 e/Å^3, which

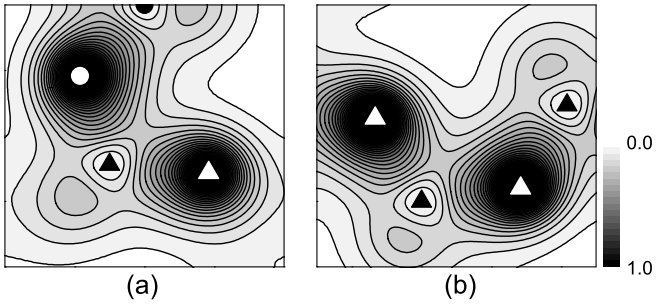

FIG. 4: Valence charge density maps of BeH_2 where (a) is the plane established by the three labeled atoms (1 to 3) as shown in Fig. 1 and (b) is the (001) plane. Here • stands for Be1, ▲ for Be2, ○ for H1 and △ for H2. The contour lines are drawn from 0.0 to 1.0 at 0.05 ev/Å^3 intervals.

is prominently higher than that in typical ionic crystals. This values is also much larger than that in isoelectroic MgH_2 system. In fact, our calculation on MgH_2 gave charge density of 0.17 e/Å^3 at the midpoint of the Mg−H bond, which is comparable well with recent experimental data[18] of 0.2 e/Å^3. Thus again, the charge distribution reveals that hydrogen is more strongly bonded to Be in BeH_2 than to Mg in MgH_2. As a result, the calculated Be−H bond length (∼1.37 Å, see Table I) is remarkably smaller than the Mg−H bond length (1.93 Å). Although hydrogen atoms do not form bond, for illustration, here we also present the charge densities at the midpoint in the line that links the nearest-neighbor H atoms, which are ∼0.2 e/Å^3 for BeH_2 and ∼0.15 e/Å^3 for MgH_2. Interestingly, the nearest-neighbor H-H distance in BeH_2 is also larger than that in MgH_2 by ∼0.25 Å.

From above results, now it becomes clear that the bonding nature of hydrogen in BeH_2, including the ionicity and covalency, is even more complex than in MgH_2. Specially, because of complicated charge transfer process, which involves not only ionic but also covalent charge redistribution, one may wonder how to characterize the valency of H and Be in BeH_2. Without knowing more appropriate way to valency, here we define and determine the so-called ionic radii of H and Be by using the method raised by Yu and Lam[19] in studying MgH_2. In this way, H ionic radius is defined as the half of average nearest-neighbor H-H distance. Subtracting the H ionic radius from the average nearest-neighbor Be-H distance gives the ionic radius of Be. Thus the ionic radius of H in our system is 1.131 Å and 0.237 Å for Be ions. After integration, we find 0.005 electrons around Be and 1.631 electrons around H. As a result, the valency of Be and H are represented as $Be^{1.99+}$ and $H^{0.63-}$. For MgH_2 our calculations give the valency of Mg and H as $Mg^{1.95+}H^{0.60-}$. Clearly, our calculated valency shows that compared to the MgH_2 system, charge transfer process is more prominent in BeH_2 system. Therefore, we would like to derive that the the definition of ionic radius by Yu and Lam still works for more covalent BeH_2 hydride.

IV. CONCLUSION

In summary, we have investigated the structural, mechanical, electronic, and chemical bonding properties of BeH_2 through first-principles DFT-GGA calculations. The calculated structural parameters are in good agreement with available experimental results. We have calculated the nine independent elastic constants and our results well obey the mechanical stability criteria. In particular, the calculated C_{12} and C_{23} are negligibly small, and C_{13} is much smaller than C_{11} or C_{33}. The bulk modulus B, shear modulus G, Young's modulus E and Poisson's ratio v have been obtained based on the knowledge of the elastic constants. The bonding nature of hydrogen in BeH_2 have been fully analyzed in terms of the band structure, density of state, and valence charge distribution. It has been shown that the Be−H bond displays a mixed ionic/covalent character. Here the ionicity is mainly featured by charge transfer from Be $2s$ to H $1s$ states, while the covalency is manifested by prominent hybridization of H $1s$ and Be $2p$ states. The elemental valency in BeH_2 has been determined to be $Be^{1.99+}$ and $H^{0.63-}$. By a systematic comparison, it has been shown that the chemical bonding nature of hydrogen in BeH_2 is even more complex than in MgH_2.

* To whom correspondence should be addressed. Electronic address: zhang_ping@iapcm.ac.cn

[1] D. A. Armstrong, J. Jamieson, and P. G. Perkins, Theor. Chim. Acta. **51**, 163 (1979).
[2] G. S. Smith, Q. C. Johnson , D. K. Smith, D. E. Cox, R. L. Snyder, and R. S. Zhou, Solid. State. Commun. **67**, 491 (1988).
[3] P. Vajeeston, P. Ravindran, A. Kjekshus, and H. Fjellvåg, Appl. Phys. Lett. **84**, 34 (2004).
[4] U. Hantsch, B. Winkler, and V. Milman, Chen. Phys. Lett. **378**, 343 (2003).
[5] M. Ahart, J. L. Yarger, K. M. Lantzky, S. Nakano, H. Mao, and R. J. Hemley, J. Chem. Phys. **124**, 014502 (2006).
[6] G. Kresse and J. Furthmüller, Phys. Rev. B **54**, 11169 (1996).
[7] P. E. Blöchl, Phys. Rev. B **50**, 17953 (1994).
[8] J. P. Perdew, K. Burke, and Y. Wang, Phys. Rev. B **54**, 16533 (1996).
[9] H. J. Monkhorst and J. D. Pack, Phys. Rev. B **13**, 5188 (1972).
[10] J. F. Nye, *Physical Properties of Crystals* (Oxford University Press, 1985).

[11] W. Voigt, *Lehrburch der Kristallphysik* (Teubner, Leipzig, 1928).
[12] A. Reuss and Z. Angew, Math. Mech. **9**, 49 (1929).
[13] R. Hill, Phys. Soc. London **65**, 350 (1952).
[14] J. P. Watt, J. Appl. Phys. **50**, 6290 (1979).
[15] P. Ravindran, L. Fast, P. A. Korzhavyi, B. Johansson, J. Wills, and O. Eriksson, J. Appl. Phys. **84**, 4891 (1998).
[16] R. S. Lakes, Nature (London) **358**, 713 (1992).
[17] P. Vajeeston, P. Ravindran, A. Kjekshus, and H. Fjellvåg, Phys. Rev. Lett. **89**, 175506 (2002).
[18] T. Noritake, M. Aoki, S. Towata, Y. Seno, Y. Hirose, E. Nishibori, M. Takata, and M. Sakata, Appl. Phys. Lett. **81**, 2008 (2002).
[19] R. Yu and P. K. Lam, Phys. Rev. B **37**, 8730 (1988).
[20] B. Pfrommer, C. Elsässer, and M. Fähnle Phys. Rev. B **50**, 5089 (1994).